Molecular Plant Pathology

MOLECULAR PLANT PATHOLOGY (2016) 17(4), 601–613 DOI: 10.1111/mpp.12305

Role of DetR in defence is critical for virulence of *Xanthomonas oryzae* pv. *oryzae*

MINH-PHUONG NGUYEN[1,2], JONGCHAN PARK[1,2], MAN-HO CHO[1] AND SANG-WON LEE[1,2,*]

[1]*Department of Genetic Engineering and Graduate School of Biotechnology, Kyung Hee University, Yongin 446-701, South Korea*
[2]*Institute of Crop Biotechnology, Kyung Hee University, Yongin 446-701, South Korea*

SUMMARY

Like other bacteria, *Xanthomonas oryzae* pv. *oryzae* (*Xoo*), the causal agent of bacterial leaf blight disease in rice, possesses intracellular signalling systems, known as two-component regulatory systems (TCSs), which regulate pathogenesis and biological processes. Completion of the genome sequences of three *Xoo* strains has facilitated the functional study of genes, including those of TCSs, but the biological functions of most *Xoo* TCSs have not yet been uncovered. To identify TCSs involved in *Xoo* pathogenesis, we generated knockout strains lacking response regulators (RRs, a cytoplasmic signalling component of the TCS) and examined the virulence of the RR knockout strains. This study presents a knockout strain (*detR*$^{-}$) lacking the *PXO_04659* gene which shows dramatically reduced virulence relative to the wild-type. Our studies to elucidate *detR* function in *Xoo* pathogenesis revealed a reduction in extracellular polysaccharide (EPS), intolerance to reactive oxygen species (ROS) and deregulation of iron homeostasis in the *detR*$^{-}$ strain. Moreover, gene expression of regulatory factors, including other RRs and transcription factors (TFs), was altered in the absence of DetR protein, as determined by reverse transcription-polymerase chain reaction (RT-PCR) and/or real-time quantitative RT-PCR analyses. All evidence leads to the conclusion that DetR is essential for *Xoo* virulence through the regulation of the *Xoo* defence system including EPS synthesis, ROS detoxification and iron homeostasis, solely or cooperatively with other regulatory factors.

Keywords: DetR (Detoxifying Regulator), reactive oxygen species, response regulator, two-component regulatory system, *Xanthomonas oryzae* pv. *oryzae*.

INTRODUCTION

Xanthomonas oryzae pv. *oryzae* (*Xoo*) is one of the most serious rice pathogens causing bacterial leaf blight disease, resulting in damage to this crop throughout the world. *Xoo* is a vascular pathogen that causes disease by invading through hydathodes or wounds on rice leaves, colonizing xylem vessels, and inducing wilt, yellowing and drying of leaves. Research on *Xoo* pathogenesis performed over several decades has identified many *Xoo* virulence factors (VFs), such as diffusible signal factors (DSFs) (He *et al*., 2010), extracellular polysaccharides (EPSs) (Kim *et al*., 2009), lipopolysaccharides (LPSs) (Li and Wang, 2011), adhesins (Das *et al*., 2009), a type 2 secretory system (T2SS) (Ray *et al*., 2000), extracellular degradative enzymes (Jha *et al*., 2007), a type 3 secretory system (T3SS) (Cho *et al*., 2008) and T3SS effectors (White *et al*., 2009). Mutation in any of these VFs results in virulence deficiency in *Xoo*.

Two-component regulatory systems (TCSs) are intracellular signal transduction systems that control *Xoo* biological processes and pathogenesis. A typical TCS contains a histidine kinase (HK) and a cognate response regulator (RR) (West and Stock, 2001) whose genes are often paired in an operon. HKs normally have sensor, dimerization and ATPase domains. RRs consist of receiver and effector domains. A typical signal transduction scheme for TCSs is as follows. After being triggered by stimuli, the HK dimer is autophosphorylated at the conserved histidine (His) in its dimerization domain with the aid of the ATPase domain (West and Stock, 2001). The receiver domain of the RR transfers a phosphoryl group from the phosphorylated HK to its conserved asparagine (Asp) residue. The effector domain can then generate output response by interacting with DNA, RNA or protein, or by functioning as an enzyme (West and Stock, 2001). In addition to the typical scheme, conduits among TCS pathways, including cross-talk, cross-regulation and branched pathways, also exist (Laub and Goulian, 2007). TCSs have been systematically annotated by bioinformatics analysis in three completely sequenced *Xoo* genomes (Lee *et al*., 2005; Ochiai *et al*., 2005; Salzberg *et al*., 2008) and the data can be found in the Prokaryotic TCS database (P2CS: http://www.p2cs.org) (Barakat *et al*., 2011). Each *Xoo* genome encodes a large number of TCS genes that account for approximately 3% of the total nucleotide sequence of these genomes, higher than the estimated average number (approximately 2%) for other bacteria (Wang *et al*., 2010). However, the biological functions of *Xoo* TCSs are poorly understood. The functions of only four RRs and their cognate HKs (ColR, PhoP, RaxR and VieA) have been directly clarified in *Xoo* (Burdman *et al*., 2004; Lee *et al*., 2008b; Liang *et al*., 2011; Subramoni *et al*., 2012).

*Correspondence: Email: swlee6803@khu.ac.kr

Our group aimed to identify novel RRs controlling *Xoo* pathogenesis and to clarify the biological processes under their control. First, knockout mutant strains for most of the PXO99 (a Philippine race 6) RRs [including hybrid histidine kinase-response regulator (HyHK)] were generated based on information from the P2CS database, and the virulence of the mutants was examined by virulence assays. Second, several experiments focusing on known VFs with mutant strains selected from the virulence assays were carried out to determine the function of the RRs in *Xoo* virulence. Moreover, we compared the transcription levels of other RRs and transcription factors (TFs) between the PXO99 and RR knockout strains *in planta* to explore the relationship between the identified RRs and other regulatory factors. In this study, we report a gene (*detR*, *det*oxifying *r*egulator) encoding an RR protein and its involvement in *Xoo* virulence.

RESULTS

Virulence is impaired in the *detR*⁻ strain

Among the generated RR knockout strains, one strain carrying insertion of a kanamycin resistance cassette at nucleotide 105 of the open reading frame (ORF) of gene *PXO_04659* (Fig. S1A, see Supporting Information) showed dramatically decreased lesion length on Taipei 309 (TP309, a Japonica rice variety that is susceptible to PXO99) leaves in virulence assays compared with PXO99 (1.8 ± 0.8 cm vs. 14.3 ± 1.6 cm, respectively; Fig. 1A, C). A complementary strain of *detR*⁻ constitutively expressing the DetR protein (see Methods S1), C*detR*⁻ (Fig. S2, see Supporting Information), restored 90% of virulence (13.8 ± 1.5 cm) compared with PXO99 (Fig. 1A, C). We then examined the average of the bacterial population of each strain per square centimetre (cm^2) of area of infected leaves at 14 days post-inoculation (dpi). Although the starting populations of the strains binding to each leaf were very similar [approximately 10^3 colony-forming units (CFU)/cm^2], the population of *detR*⁻ at 14 dpi (~10^2 CFU/cm^2) was markedly smaller than that of PXO99 and C*detR*⁻ (~10^6 CFU/cm^2) (Fig. 1B). This result indicates that DetR is critical for *Xoo* virulence and proliferation in host conditions.

The production of EPS is decreased in *detR*⁻

Colonies of *detR*⁻ appeared smaller and drier than those of PXO99 and C*detR*⁻ on peptone sucrose agar (PSA) medium (Fig. 2A), which might be caused by either reduced cell number and/or reduced production of EPS in *detR*⁻. Therefore, growth curves of PXO99 and *detR*⁻ in rich peptone sucrose broth (PSB) medium were established to examine the dynamics of bacterial population sizes during 4 days (see Methods S2). It was shown that *detR*⁻ exhibited similar dynamics of bacterial population size to PXO99 up to 4 days after incubation (Fig. S3A, see Supporting Information), although the population sizes of *detR*⁻ on the third and fourth days after incubation seemed to be slightly smaller than those of PXO99. However, they were not significantly different based on a Student's *t*-test at $P < 0.01$. As a complementary test, the average CFU per colony was measured at 3, 4 and 5 days after inoculation for strains grown during the same period of time on PSA (see Methods S3). No differences were quantified (Fig. S3B). EPS production was then measured in PXO99, *detR*⁻ and C*detR*⁻ strains by the sulfuric–phenol colorimetric method (Kumar and Sakthivel, 2001). This assay indicated that EPS production in *detR*⁻ (580 ± 32 μg/mL culture) was reduced by almost 50% compared with that in PXO99 (1146 ± 117 μg/mL culture) (Fig. 2B). The expression levels of three representative genes among 12 reported *gum* genes for EPS expression (Kim *et al.*, 2009) in PXO99 and

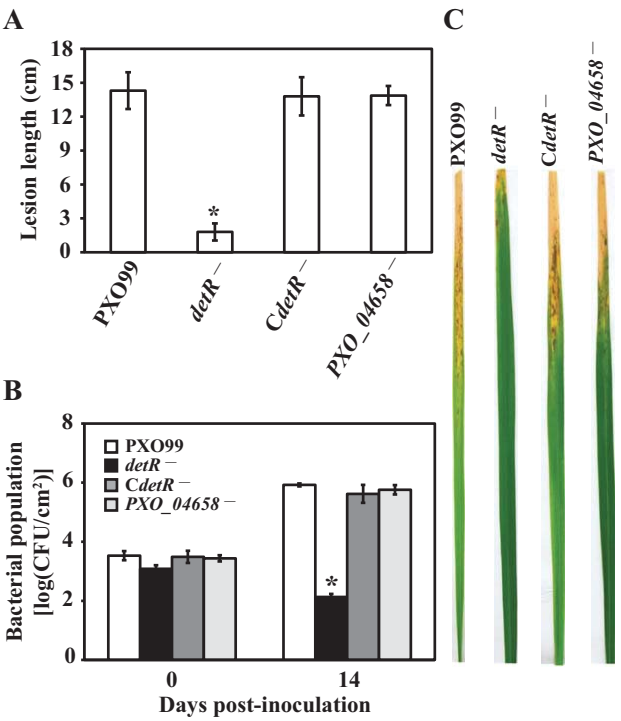

Fig. 1 Virulence phenotypes of PXO99, *detR*⁻, C*detR*⁻ and *PXO_04658*⁻ strains. (A) Length of lesions caused by PXO99, *detR*⁻, C*detR*⁻ and *PXO_04658*⁻ on TP309 rice leaves at 14 dpi (days post-inoculation). Rice leaves were inoculated with 10^7 colony-forming units (CFU)/mL of bacterial suspension by the scissor clipping method. Bars are mean ± standard deviation (SD) ($n = 20$). * indicates that the lesion length of *detR*⁻ was significantly lower than that of PXO99, C*detR*⁻ and *PXO_04658*⁻ by Duncan test ($P < 0.01$). (B) Bacterial populations in leaves at 0 and 14 dpi. Immediately after infection and at 14 dpi, 1- and 25-cm^2 samples from the infected site of three leaves were used to extract bacteria. Bars are mean ± SD ($n = 3$). * indicates that the population of *detR*⁻ was significantly smaller than that of PXO99, C*detR*⁻ and *PXO_04658*⁻ by Duncan test ($P < 0.05$). (C) Representative images of TP309 leaves inoculated with the various strains at 14 dpi. The photographs were taken at a resolution of 180 dots per inch. All experiments were repeated three times with high consistency, and results from one experiment are shown.

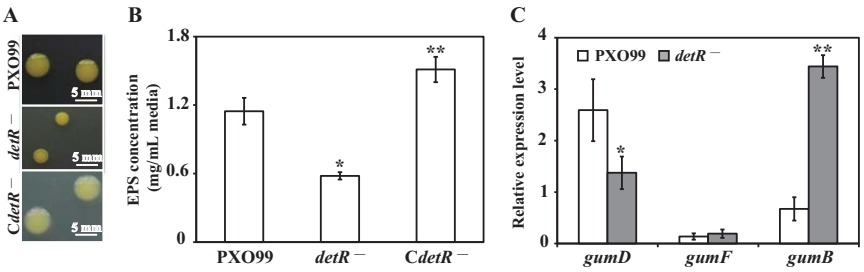

Fig. 2 Extracellular polysaccharide (EPS) production of PXO99, *detR*⁻ and C*detR*⁻. (A) Colonies of PXO99, *detR*⁻ and C*detR*⁻ on peptone sucrose agar (PSA) at 3 days after incubation. Photographs were taken at a resolution of 180 dots per inch. (B) Quantification of EPS production by *Xanthomonas oryzae* pv. *oryzae* (*Xoo*) strains in tryptone–glucose yeast (TGY) medium. EPS was extracted from the supernatant of 5-day-old bacterial cultures using ethanol precipitation and measured by the sulfuric–phenol colorimetric method at 490 nm. Bars are mean ± standard deviation (SD) ($n = 3$). * indicates that EPS production of *detR*⁻ was significantly lower than that of PXO99 by Duncan test ($P < 0.05$). ** indicates that EPS production of C*detR*⁻ was significantly higher than that of PXO99 by Duncan test ($P < 0.05$). (C) Relative expression of *gumD*, *gumF* and *gumB* in PXO99 and *detR*⁻. RNA samples were extracted from TGY culture at stationary phase by RNAiso and 40 ng of cDNA was used for real-time quantitative reverse transcription-polymerase chain reaction (qRT-PCR). *16S rRNA* was used as a reference gene in each experiment. Bars are mean ± SD ($n = 3$). * indicates that gene expression in *detR*⁻ was significantly lower than that in PXO99 by Student's *t*-test ($P < 0.05$). ** indicates that gene expression in *detR*⁻ was significantly higher than that in PXO99 by Student's *t*-test ($P < 0.05$). All experiments were repeated three times with high consistency, and the results from one experiment are presented.

detR⁻ strains were then tested in tryptone–glucose yeast (TGY) medium by real-time quantitative reverse transcription-polymerase chain reaction (qRT-PCR). Although *gumF* showed no difference and *gumB* was upregulated in *detR*⁻, the expression of *gumD* was significantly downregulated in *detR*⁻ (Fig. 2C). This agrees with a previous report indicating that mutations in *gumD* abolished EPS synthesis because GumD is the enzyme responsible for the first step of the EPS biosynthetic process (Becker *et al*., 1998; Katzen *et al*., 1998). These results suggest that DetR regulates EPS synthesis in *Xoo* via *gumD* expression.

detR⁻ overproduces siderophores in iron-rich conditions

Mutations in some of the genes associated with iron homeostasis have been reported to cause virulence deficiency in *Xoo* (Chatterjee and Sonti, 2002; Pandey and Sonti, 2010; Subramoni and Sonti, 2005; Subramoni *et al*., 2012). The amount of siderophores in *detR*⁻ was investigated under iron-rich and iron-limited conditions to test whether a change in iron homeostasis could be associated with the reduced virulence of *detR*⁻. There was no significant difference in the size of the halo zone between the three strains in iron-limited conditions [PSA-chromeazurol S (CAS) containing 100 μM of the iron chelator 2,2'-dipyridyl (PSA-CAS-DP)], implying similar secretion of siderophores in these strains (Fig. 3A, B). However, the diameter of the halo zone of *detR*⁻ on iron-rich plates [PSA containing 0.1 mM CAS and 9 μM Fe^{3+} (PSA-CAS)] was markedly greater than that of PXO99 and C*detR*⁻ (Fig. 3A, B). This result indicates that *detR*⁻ overproduces siderophores in iron-rich conditions relative to PXO99 and C*detR*⁻. Consequently, we checked the expression levels of genes reported to be involved in iron homeostasis or their homologues in PXO99. The genes tested were ferric uptake regulators (*fur1* and *fur2*), a TCS involved in colonization (*colRS*), a ferrous uptake transporter (*feoB*), three representative siderophore synthesis genes (*xssA*, *xssB* and *xssE*) and TonB-dependent outer membrane receptor (*xsuA*) (Pandey and Sonti, 2010; Subramoni and Sonti, 2005; Subramoni *et al*., 2012). RT-PCR performed to determine differences in gene expression between PXO99 and *detR*⁻ gave unclear results (Fig. S4A, see Supporting Information); therefore, we examined the expression of selected genes by real-time qRT-PCR (Fig. 3C). Remarkably, genes involved in siderophore synthesis (*xss*) and iron uptake (*feoB*, *xsuA*) were upregulated in *detR*⁻ in both conditions, suggesting that the phenotype of *detR*⁻ in the siderophore assay was caused by expression changes in these genes. Moreover, the regulatory genes (*fur1* and *fur2*) were also upregulated in *detR*⁻, suggesting that *detR*⁻ might try to maintain iron homeostasis via the overexpression of these regulatory proteins.

The *detR*⁻ cell population was reduced in iron-rich conditions to a greater extent and earlier than that of PXO99

Deregulation of iron homeostasis generally results in severe defects in bacterial growth (Chatterjee and Sonti, 2002; Pandey and Sonti, 2010; Subramoni and Sonti, 2005; Subramoni *et al*., 2012). Growth curves of *detR*⁻ were established in iron-rich and iron-limited conditions to test whether an imbalance in iron homeostasis has an adverse effect on the growth pattern. After the three strains similarly reached the stationary phase on the second day after incubation, the population of *detR*⁻ decreased exponentially on the third and fourth days, whereas PXO99 and C*detR*⁻ maintained their population sizes until the third day and decreased on the fourth day in iron-rich conditions (PSB containing 9 μM $FeCl_3$) (Fig. 4A). In the

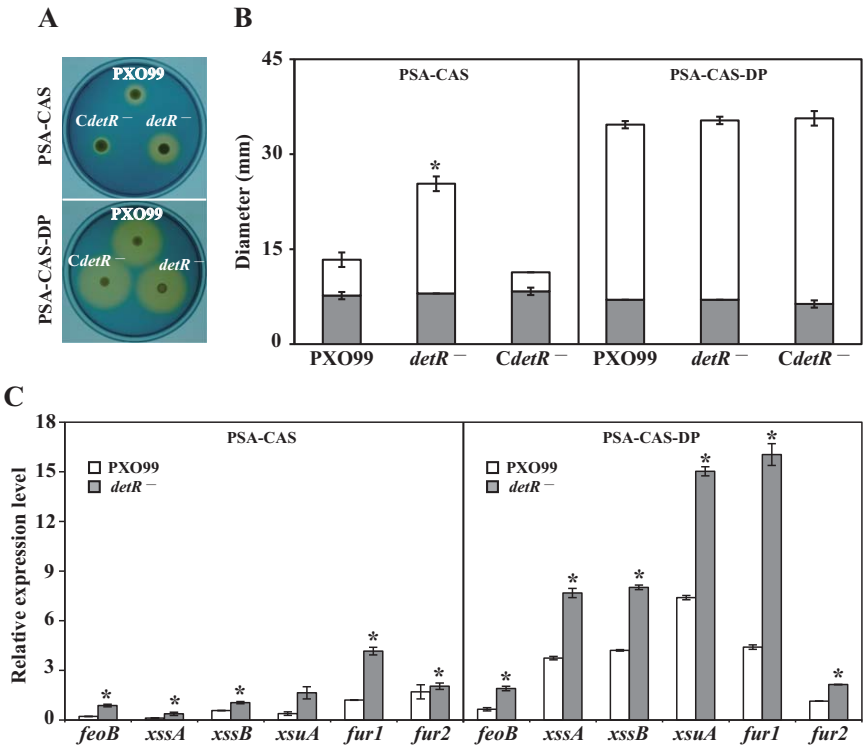

Fig. 3 Siderophore assay of PXO99, *detR*⁻ and C*detR*⁻. (A) Siderophore assay of *Xanthomonas oryzae* pv. *oryzae* (*Xoo*) strains on iron-rich [peptone sucrose agar-chromeazurol S (PSA-CAS)] and iron-limited [PSA-CAS containing 100 μM of the iron chelator 2,2'-dipyridyl (PSA-CAS-DP)] conditions. Bacterial suspensions [10 μL, 10^8 colony-forming units (CFU)] were dropped onto the plates. Images were taken after 2 days for PSA-CAS and 1 day for PSA-CAS-DP at a resolution of 180 dots per inch. (B) Comparison of halo zone diameters of each strain after 2 days for PSA-CAS and 1 day for PSA-CAS-DP. Bars are mean ± standard deviation (SD) ($n = 3$). Open bar, halo zone diameter. Grey bar, drop diameter. * indicates that the halo zone of *detR*⁻ was significantly larger than that of PXO99 by Duncan test ($P < 0.01$). (C) Relative expression of genes involved in siderophore synthesis (*xssA*, *xssB*), iron uptake (*feoB*, *xsuA*) and ferric uptake regulator (*fur*) in PXO99 and *detR*⁻. RNA samples were extracted from bacteria grown on PSA-CAS and PSA-CAS-DP plates after 2 days using RNAiso and 40 ng of cDNA were used for real-time quantitative reverse transcription-polymerase chain reaction (qRT-PCR). *16S rRNA* was used as a reference gene in each experiment. Bars are mean ± SD ($n = 3$). * indicates that gene expression in *detR*⁻ was significantly higher than that in PXO99 strains by Student's *t*-test ($P < 0.05$). All experiments were repeated three times with high consistency, and results from one experiment are presented.

meantime, populations of PXO99, *detR*⁻ and C*detR*⁻ were very similar and did not decrease until the fourth day in iron-limited conditions (Fig. 4B). This result suggests that *detR*⁻ might continuously take up iron because of the overexpression of genes involved in siderophore synthesis and iron uptake (Fig. 3C), leading to metal toxicity similar to, but not as dramatic as, that observed for a *fur* mutant (Subramoni and Sonti, 2005).

detR⁻ is hypersensitive to hydrogen peroxide (H_2O_2) as a result of reduction and deregulation of catalase activity

During the early stages of infection, phytopathogens have to survive under reactive oxygen species (ROS) bursts generated by the host plant (Dat *et al*., 2000). The remarkable reduction in the *detR*⁻ population in the initial hours post-infection (within 3 hpi; Fig. S5, see Supporting Information) suggests that *detR*⁻ might have weak viability under ROS bursts in plant tissue. To examine the tolerance of *detR*⁻ to a high concentration of ROS, we treated PXO99, *detR*⁻ and C*detR*⁻ with various concentrations of H_2O_2 (0.5, 1, 5, 10 mM) for 1 h. The *detR*⁻ mutant was much less tolerant than PXO99, even at the lowest H_2O_2 concentration (0.5 mM) (Fig. 5A). No *detR*⁻ colonies were detected at approximately 8.5 mM H_2O_2, whereas PXO99 survived at very high concentrations of H_2O_2 (140 mM) (Fig. S6, see Supporting Information). Clearly, the mutation in *detR* seriously disrupts the tolerance of *Xoo* to oxidative stress.

To identify why *detR*⁻ was intolerant to H_2O_2, we examined the activity of catalase, the main enzyme in the H_2O_2 detoxification of *Xoo* (Chamnongpol *et al*., 1995). *Xoo* strains were cultured to the early logarithmic phase in PSB, when the amount of catalase produced is highest (Chamnongpol *et al*., 1995), and catalase activity was tested (Aebi, 1974). The catalase activity of *detR*⁻ was much lower than that of PXO99 and C*detR*⁻ without H_2O_2 treatment (Fig. 5B). Exposure to 0.5 mM H_2O_2 did not increase catalase activity in *detR*⁻, whereas that of PXO99 increased two-fold compared with

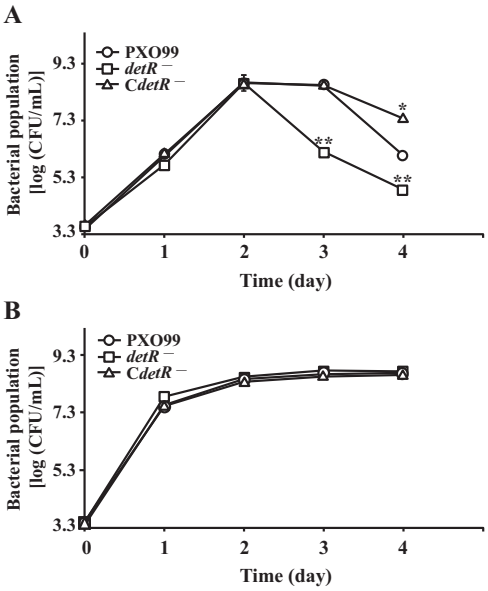

Fig. 4 Growth curves of PXO99, *detR*⁻ and C*detR*⁻ under different iron conditions. Bacteria [approximately 10^3 colony-forming units (CFU)/mL] were inoculated in 50 mL peptone sucrose broth (PSB) containing 9 μM $FeCl_3$ (A) or 100 μM 2,2'-dipyridyl (DP) (B), and cultured at 28 °C for 4 days. The bacterial population was quantified every 24 h. The experiments were performed twice with similar results. Bars are mean ± standard deviation (SD) ($n = 4$). * and ** indicate that *detR*⁻ and C*detR*⁻, respectively, were significantly different from PXO99 by Duncan test ($P < 0.01$).

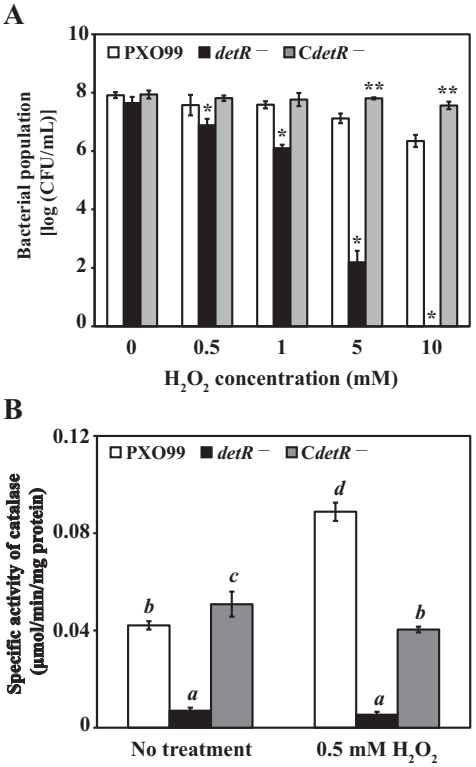

Fig. 5 Tolerance of oxidative stress and catalase activity of PXO99, *detR*⁻ and C*detR*⁻. (A) Tolerance of *Xanthomonas oryzae* pv. *oryzae* (*Xoo*) strains to various concentrations of H_2O_2. Bacteria in peptone sucrose broth (PSB) [10^8 colony-forming units (CFU)/mL] were treated with various concentrations of H_2O_2 for 1 h, washed and dropped onto peptone sucrose agar (PSA) plates to quantify the population. The results were consistent between three repeated experiments with five technical replicates for each sample. Bars are mean ± standard deviation (SD). * indicates that the population of *detR*⁻ was significantly lower than that of PXO99 by Duncan test at $P < 0.001$. ** indicates that the population of C*detR*⁻ was significantly greater than that of PXO99 by Duncan test at $P < 0.001$. (B) Specific activity of catalase. Bacteria were cultured in 300 mL of PSB for 2 h to the early logarithmic phase. Bacteria were then harvested and total proteins were extracted. Catalase activity was assayed from the rate of H_2O_2 decomposition as measured by decreased absorbance at 240 nm. The reaction mixture contained 50 mM potassium phosphate buffer (pH 7.0) and 100 μg of total protein extract. The experiments were performed twice with three technical replicates per sample. Bars are mean ± SD. Different letters indicate significant differences among samples by Duncan test at $P < 0.05$.

the non-treatment condition (Fig. 5B). Therefore, the reduction and deregulation of detoxification by catalase results in the H_2O_2 intolerance of *detR*⁻. The absence of restoration of the wild-type phenotype in C*detR*⁻ with treatment of H_2O_2 might be caused by the use of a non-native promoter (*lacZ*) for DetR in this strain.

Mutation in *detR* induces changes in transcriptional levels of VFs and other regulatory genes *in planta*

To examine whether defects in VFs contribute to the defective virulence in *detR*⁻, we tested the expression levels of well-known VFs *in planta*. PXO99 and *detR*⁻ strains were extracted from infected leaves at 6 dpi for RT-PCR or real-time qRT-PCR analyses (Figs 6A and S4) using specific primers listed in Table S2. All three *gum* genes tested were strongly reduced in *detR*⁻, suggesting that DetR positively regulates *gum* genes during infection. Among other VFs, the expression of *rpfB* was significantly decreased and that of *hrpX* and *hrpD5* was increased in *detR*⁻ (Fig. 6A). The expression of the other genes (*T2SS*, *LPS* and adhesion-related genes) was not significantly affected in *detR*⁻ (Fig. S4B). Overall, these findings indicate that knockout of *detR* alters the expression of other virulence-associated genes, including those involved in the synthesis of DSF and T3SS.

The expression levels of 59 RRs (including HyHKs) and 75 TFs in PXO99 and *detR*⁻ *in planta* were compared to investigate the gene expression of other regulatory proteins in the absence of DetR (used primers for this analysis are listed in the Table S3 and S4). Most of the RR and TF genes showed insignificant changes in the mutant strain under the tested conditions (Figs S7 and S8, see Supporting Information). However, four RRs and TFs (*PXO_00057*, *cheB*; *PXO_03078*; *PXO_01183*; *PXO_00244*) were clearly downregulated (Fig. 6B) and 17 were upregulated in the mutant, as shown in Fig. 6C. These results indicate that DetR may functionally cooperate with other regulatory factors (RRs and TFs).

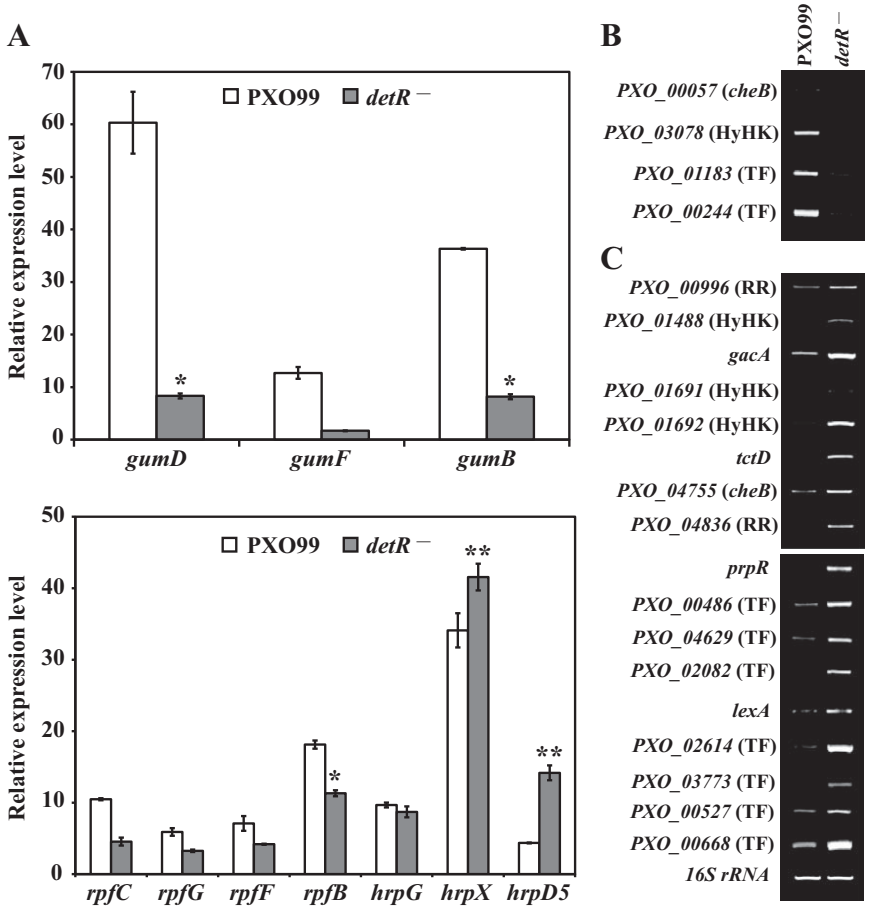

Fig. 6 Gene expression of virulence factors (VFs), response regulators (RRs) and transcription factors (TFs) of PXO99 and *detR*⁻ *in planta*. (A) Relative expression of VF genes in PXO99 and *detR*⁻. Bacteria were harvested from infected leaves at 6 days after infection. RNA samples were extracted using RNAiso, and real-time quantitative reverse transcription-polymerase chain reaction (qRT-PCR) was carried out with 40 ng of the synthesized cDNA. *16S rRNA* was used as a reference gene in each experiment. The experiments were repeated three times with three technical replicates. Bars are mean ± standard deviation (SD). * indicates that gene expression in *detR*⁻ was significantly lower than that in PXO99 by Student's *t*-test ($P < 0.05$). ** indicates that gene expression in *detR*⁻ was significantly higher than that in PXO99 by Student's *t*-test ($P < 0.05$). (B, C) RT-PCR of genes encoding RRs and TFs expressed dominantly in PXO99 (B) and *detR*⁻ (C) *in planta*. *16S rRNA* was used as an internal control for all experiments. The experiments were repeated three times and the results shown are from one representative experiment. Photographs were taken at a resolution of 96 dots per inch.

Lack of an adjacent gene encoding an HK did not change *Xoo* virulence

A putative HK gene (*PXO_04658*) located 196 nucleotides downstream of *detR* could be the cognate HK of DetR (Fig. S1A, B). Therefore, we analysed the 196-nucleotide region between *detR* and *PXO_04658* by BPROM (Solovyev and Salamov, 2011) to check for possible promoter regions. This region is predicted to contain promoter elements (–35 box, a –10 box and two TF binding sites) (Fig. S1A), implying that *PXO_04658* is not in the same operon as *detR*. However, the possibility that PXO_04658 is the cognate HK of DetR could not be excluded. Therefore, the HK knockout strain (*PXO_04658*⁻) was generated by replacing a region from nucleotides 649 to 820 of the gene ORF with a kanamycin resistance cassette. The length of the lesions caused by *PXO_04658*⁻ on TP309 leaves (13.8 ± 2 cm) was similar to that induced by PXO99 (Fig. 1A, C). This finding was confirmed by the bacterial population proliferation in 1 cm^2 of infected leaves at 14 dpi (Fig. 1B). Moreover, *PXO_04658*⁻ was similar to the wild-type in other experiments, including EPS production, siderophore production and H_2O_2 tolerance (Fig. S9, see Supporting Information). These findings suggest that DetR might be an orphan RR that does not have a cognate HK, or that *detR* has *PXO_04658* as a cognate HK gene, but detR can be somehow expressed and activated in the absence of PXO_04658 by other HKs.

DISCUSSION

We have carried out a genome-scale mutagenesis to identify *Xoo* RR mutants that exhibit impaired virulence in TP309 rice. *detR*⁻ is one of the mutants that showed dramatically reduced virulence. The results of this study indicate that defects in the defence system, including reduced EPS production, deregulation of ROS detoxification and impaired iron homeostasis, are major causes of the deficiency in virulence of *detR*⁻.

Reduction of EPS caused by the reduced expression of *gumD* decreases the protective and pathogenic abilities of *detR*⁻ because EPS is known to be not only a basal defence factor, but also a VF of *Xoo*. EPS is a polymer of repeating pentasaccharide units, with a cellulose backbone and trisaccharide side chains, that is strongly produced when bacteria grow in conditions containing carbon sources, such as glucose, sucrose, maltose, cellobiose, mannose and xylose (Jansson *et al*., 1975; Vojnov *et al*., 2001). As the polymer is highly hydrated, it protects bacteria from desiccation and hydrophobic bacteriostatic compounds in the air-filled plant intercellular space (Shen and Ronald, 2002). In addition, EPS

enhances pathogenic capability because it facilitates *Xoo* attachment to leaf surfaces, blocks the xylem vessels and suppresses basal defences in plant cell walls, such as callose deposition (Aslam *et al*., 2008; Branda *et al*., 2005; Denny, 1995; Sutherland, 2001; Yun *et al*., 2006). A reduction of EPS as the consequence of mutations in *gum* genes responsible for EPS synthesis has been reported previously to cause virulence deficiency in *Xoo* (Kim *et al*., 2009). There are 12 *gum* genes, *gumB* to *gumM*, and each contributes differently to EPS production (Kim *et al*., 2009). Listed in temporal order of function, these genes are as follows: *gumD*, *gumM*, *gumH*, *gumK* and *gumI* for the biosynthesis of the pentasaccharide repeating unit; *gumF*, *gumG* and *gumL* for modification of the pentasaccharide repeating unit; and *gumB*, *gumC*, *gumE* and *gumJ* for polymerization and transport (Kim *et al*., 2009). Mutations of *gum* genes participating in the modification of pentasaccharide units do not affect the ability to produce EPS and maintain virulence. However, mutations of *gum* genes involved in pentasaccharide unit synthesis (*gumD*, *gumM*, *gumH*, *gumK*) or polymerization and transport (*gumB*, *gumC*, *gumE*) reduce EPS production by 70% and dramatically decrease virulence. In particular, mutation of *gumD* abolishes EPS because GumD is the first enzyme in the EPS biosynthesis process (Becker *et al*., 1998; Katzen *et al*., 1998). The results of this study (Figs 2 and 6A) indicate that *detR*$^-$ is defective in pathogenesis, partly because of a reduction in EPS as a result of *gumD* downregulation. However, the opposite expression levels of *gumF* and *gumB* in TGY compared with that *in planta* raises questions. We suppose that *gumF* and *gumB* are regulated by different regulators depending on TGY or host conditions. In addition to a promoter located upstream of *gumB* to regulate the *gum* operon, weak promoters may exist upstream of other *gum* genes to help other regulators to control regions of *gum* genes (Katzen *et al*., 1996; Lee *et al*., 2008a; Pollock *et al*., 1994; Vanderslice *et al*., 1989). Therefore, we conclude that DetR plays a key role in EPS synthesis and virulence by regulating *gumD* expression.

Another key factor associated with the reduced virulence of *detR*$^-$ is ROS intolerance caused by the deregulation of the detoxification system. The production of ROS, including superoxide (O_2^-) and H_2O_2, has been reported following pathogen recognition (Auh and Murphy, 1995; Doke, 1983; Grant *et al*., 2000). In rice, ROS can be generated in two distinct phases: (i) a non-specific phase occurring within minutes after pathogen invasion; and (ii) a specific phase with recognition of incompatible pathogens 1–3 h after the initial burst (Dat *et al*., 2000). Virulent pathogens (e.g. PXO99 for TP309 rice) that avoid host recognition induce only the non-specific phase of ROS generation (Lamb and Dixon, 1997). In our study, *detR*$^-$ was hypersensitive to H_2O_2 (Figs 5A and S6) and only a small bacterial population survived in leaves at 3 h after infection (Fig. S5), indicating that *detR*$^-$ is intolerant to the ROS burst generated in rice and is therefore killed. We measured the catalase activity of *detR*$^-$ because catalase is one of two primary enzymes (the other is superoxide dismutase) required for detoxification in *Xanthomonas* spp., especially in the early stages of infection (Chamnongpol *et al*., 1995). Our results showed that catalase activity in *detR*$^-$ was depleted and deregulated (Fig. 5B). This finding leads us to conclude that *detR*$^-$ has impaired pathogenicity because of ROS intolerance as a consequence of depletion and deregulation of detoxifying enzymes, such as catalase.

Another important factor contributing to the loss of virulence of *detR*$^-$ is the deregulation of iron homeostasis. The exact relationship between iron homeostasis and virulence is still unknown; however, it is clear that iron is directly related to redox stress and that abundant iron can interact with O_2^- and H_2O_2 to produce hydroxyl radicals that are damaging to cells (Andrews *et al*., 2003; Winterbourn, 1995). Previous reports have shown that bacteria exhibit increased sensitivity to ROS after growth under iron-rich conditions (Abdul-Tehrani *et al*., 1999; Repine *et al*., 1981), and that mutation of the *fur* gene (which results in deregulation of iron metabolism) increases sensitivity to redox stress (Touati *et al*., 1995). In our study, *detR*$^-$ exhibited siderophore overproduction as a result of the overexpression of genes involved in siderophore synthesis and iron uptake (Fig. 3C), suggesting that DetR negatively regulates these genes to minimize the production of cell-damaging agents and that mutation of *detR* results in impaired iron homeostasis. This impairment increases redox stress in mutant cells and leads to early death of the *detR*$^-$ population in iron-rich conditions (Fig. 4A). Moreover, impaired iron homeostasis renders *detR*$^-$ more sensitive to ROS generated by rice and thus results in reduced virulence. These features are similar to those of the *Xoo fur* mutant (Subramoni and Sonti, 2005); however, although the *fur* mutant exhibits slow growth in PSB, *detR*$^-$ shows a normal growth pattern similar to that of the wild-type (Fig. S3). It is possible that DetR is necessary for *Xoo* iron homeostasis, but is not as important as Fur.

Of the other VF genes studied, only the reduced expression of *rpfB* (Fig. 6A), which encodes fatty acyl-CoA ligase involved in DSF synthesis, may contribute partially to the virulence deficiency of *detR*$^-$, as mutation in *rpfB* has been reported to reduce virulence and EPS production in *Xoo* (Barber *et al*., 1997; Jeong *et al*., 2008). In the case of T3SS-related genes, *hrp* genes are overexpressed in *detR*$^-$ as a result of upregulation of *hrpX* (Fig. 6A) (Büttner and Bonas, 2010), which might be a compensational response to the serious deficiency of *detR*$^-$ pathogenicity. However, this response is not sufficiently strong to rescue the defects in the defence system described above.

In this study, we also showed that PXO_04658 is not the cognate HK of DetR because *PXO_04658* does not share an operon with *detR*, and the phenotypes of the *PXO_04658*$^-$ knockout strain are not concordant with those of *detR*$^-$ in any of our experiments (Figs 1, S5 and S9). Thus, DetR is probably an orphan RR that usually has multiple partners (Williams and Whitworth, 2010) and possibly shares signals with other RRs (Laub and

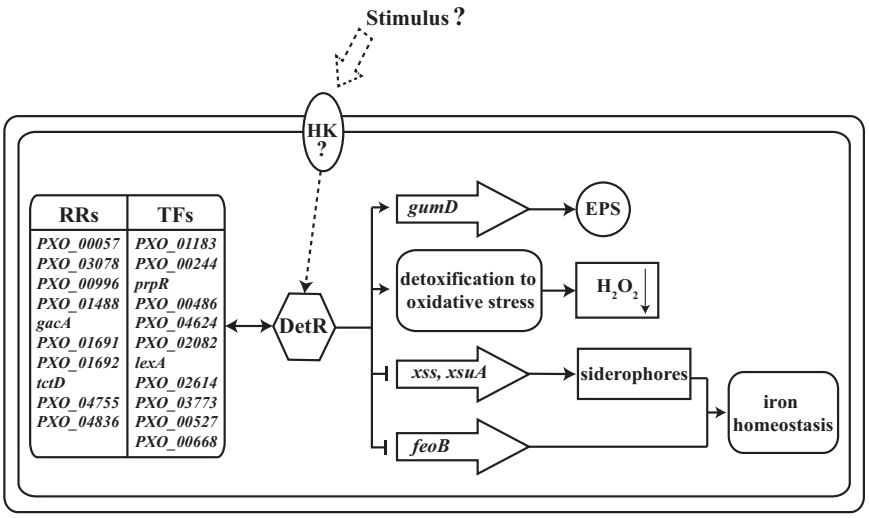

Fig. 7 Working model of the role of DetR in *Xanthomonas oryzae* pv. *oryzae* (*Xoo*). Question marks and broken arrows indicate unclarified facts in this study. Arrows indicate positive regulation. Blunt-end arrows indicate negative regulation. Two-ended arrow indicates possible interaction. EPS, extracellular polysaccharide; HK, histidine kinase; RR, response regulator; TF, transcription factor.

Goulian, 2007). The numerical disagreement between HKs (35 genes) and RRs, including HyHK (58 RR and nine HyHK genes), in the *Xoo* genome (http://www.p2cs.org) further suggests that orphan RRs, such as DetR, participate in branched signalling circuits (Laub and Goulian, 2007). To identify RRs that might share signalling pathways with DetR, we compared the gene expression levels of other RRs between PXO99 and *detR*$^{-}$. Our results showed that 10 RRs (Fig. 6B, C) exhibit altered expression in the absence of DetR. This implies that DetR may share signalling pathways with these proteins to regulate *Xoo* gene expression *in planta*.

Domain analysis of the DetR protein by SMART (Fig. S1B, C) and the classification of DetR in the P2CS database indicated that DetR is a member of the OmpR/PhoB family, the largest DNA-binding subgroup. Hence, DetR can generate specific responses by binding directly to promoter regions of target genes or through intermediate TFs. An example of cooperation between RRs and TFs has been reported in the case of the OmpR/PhoB family member HrpG, which regulates *hrp* gene expression via the HrpX TF (Büttner and Bonas, 2010). To identify possible intermediate TFs of DetR, we compared transcription levels of TFs between PXO99 and *detR*$^{-}$. We found that 11 TFs (Fig. 6B, C) showed altered expression in the absence of DetR, suggesting that DetR might interact directly or indirectly with these factors to regulate target genes.

In conclusion, DetR is involved in the regulation of critical defensive mechanisms against conditions faced by *Xoo* in rice during the early stage of infection. As shown in the model presented in Fig. 7, DetR positively controls ROS tolerance via detoxification enzymes, such as catalase. DetR also regulates *gumD* expression to synthesize sufficient EPS for protection and contributes to iron homeostasis, which is closely related to ROS sensitivity, by regulating siderophore synthesis and iron uptake genes. Furthermore, DetR might cooperate with other RRs and TFs to control *Xoo* gene expression during infection. Although further studies are needed to clarify the direct regulatory effect of DetR on these genes and the interaction of DetR with other regulatory factors, our study demonstrates the importance of the defence system in determining virulence in *Xoo* pathogenesis.

EXPERIMENTAL PROCEDURES

Biological materials and growth conditions

All bacterial strains and plasmids used in this study are listed in Table 1. *Xoo* strains were grown in PSB and TGY containing 15 μg/mL cephalexin and suitable antibiotics at 28 °C. *Escherichia coli* strains were cultured in Luria–Bertani (LB) medium at 37 °C. For both *Xoo* and *E. coli*, 25 μg/mL kanamycin, 100 μg/mL ampicillin and gentamycin (10 μg/mL for *Xoo*; 20 μg/mL for *E. coli*) were used to select transformants.

TP309 seeds [kindly donated by Dr. Jong-Seong Jeon (Institute of Crop Biotechnology, Kyung Hee University, Yongin, South Korea)] were germinated in water at 28 °C for 4 days, and then planted into soil (containing 800–2500 mg/kg of nitrogen, 50–650 mg/L of phosphoric acid, pH 4.5–5.5) and grown for 5 weeks in a glasshouse. Five-week-old plants were transferred to a growth chamber at least 2 days prior to inoculation. The chamber conditions were as follows: 14/10 h of light/dark at 28/25 °C and 80%/90% relative humidity.

Molecular techniques

Xoo genomic DNA was prepared using the method developed by Ausubel *et al*. (1994). Plasmid preparation and digestion with restriction enzymes followed standard methods described by Sambrook and Russell (2001). Sequencing of *detR* and *PXO_04658* fragments in the pGEM vector was performed using the dideoxy chain termination method with SP6 forward and T7 reverse primers. DNA, RNA and protein concentrations were measured using a Nanodrop Spectrometer ND-2000 (Thermo Scientific, Waltham, Massachusetts, USA). *Escherichia coli* transformants were produced by the heat-shock method (Froger and Hall, 2007). *Xoo* transformants were produced by electroporation, in which a mixture of 400–600 ng DNA and 10^7 CFU bacteria was electrically shocked with a

Table 1 Bacterial strains and plasmids used in this study.

Bacterial strain or plasmid	Relevant characteristics	Source or reference
Escherichia coli		
Top10	F- mcrA Δ(mrr-hsdRMS-mcrBC) φ80lacZΔM15 ΔlacX74 nupG recA1 araD139 Δ(ara-leu)7697 galE15 galK16 rpsL(Str^R) endA1 λ	Invitrogen, Waltham, Massachusetts, USA
Xanthomonas oryzae pv. *oryzae*		
PXO99Az or PXO99	Philippine race 6 strain; Cp^r	This study
detR$^-$	*PXO_04659* knockout mutant with kanamycin insertion at nucleotide 105; Cp^r and Km^r	This study
PXO_04658$^-$	*PXO_04658* knockout mutant with kanamycin insertion from nucleotide 649 to 820; Cp^r and Km^r	This study
C*detR*$^-$	*detR*$^-$ complemented with pBBR1C*detR*_N (6 × His-tag at N-terminus of DetR), Cp^r, Km^r and Gm^r	This study
Plasmid		
pGEM-Teasy	'TA' cloning vector, Am^r	Promega
pUC18	Suicide vector for generation of knockout mutant, Am^r	Clontech, Kusatsu, Shiga, Japan
pBBR1-MCS5	Broad-host-range vector for generation of complementary strains, *lacZ alpha*, Gm^r	Kovach *et al*. (1995)
pGEMKm	pGEM vector inserted by kanamycin fragment from pUC4K by *Sac*I and *Sph*I, Am^r and Km^r	This study
pGEMdetR	pGEM-Teasy vector inserted by 1159-bp *detR* fragment by TA ligation, Am^r	This study
pGEM04658	pGEM-Teasy vector inserted by 924-bp *PXO_04658* fragment by TA ligation, Am^r	This study
pUCdetR	pUC18 inserted by 1159-bp *detR* fragment from pGEMdetR (*Nde*I—*Bam*HI), Am^r	This study
pUC04658	pUC18 inserted by 924-bp *PXO_04658* fragment from pGEM04658 (*Eco*RI), Am^r	This study
pUCdetR$^-$	pUCdetR inserted by kanamycin fragment from pGEMKm (*Hin*cII), Am^r and Km^r	This study
pUC04658$^-$	pUC04658 inserted by kanamycin fragment from pGEMKm (*Mcs*I), Am^r and Km^r	This study
pGEMCdetR_N	pGEM-Teasy inserted by 765-bp *detR* fragment containing *6 × his*-tag at the forward primer by TA ligation, Am^r	This study
pBBR1CdetR_N	pBBR1-MCS5 inserted by 765-bp *6 × his-detR* fragment from pGEMCdetR_N vector (*Bam*HI-*Eco*RI), Gm^r	This study

Cp^r, Am^r, Km^r and Gm^r indicate resistance to cephalexin, ampicillin, kanamycin, and gentamycin, respectively.

Biorad Gene Pulser Xcell™ (voltage, 2.5 kV; capacitance, 25 μF; resistance, 200 Ω; cuvette, 2 mm). All primer sequences used for cloning in this study are listed in Table S1 (see Supporting Information).

Generation of *detR*$^-$ and *PXO_04658*$^-$ knockout strains

To create a vector containing a kanamycin resistance cassette with suitable restriction sites for knockout generation (pGEMKm), the kanamycin resistance cassette was subcloned from pUC4K into pGEM-Teasy vector (Promega, Fitchburg, Wisconsin, USA) by PCR with Km-F and Km-R primers, and ligated into pGEM-Teasy vector treated with *Sac*I and *Sph*I. The cassette in pGEMKm was sequenced to confirm its identity against the original sequence.

To generate *detR*$^-$ and *PXO_04658*$^-$ knockout strains, we used the marker-exchange mutagenesis method (Lee and Ronald, 2007). Specifically, the PXO99 genomic DNA template and primer sets of detR and PXO_04658 were used to clone *detR* and *PXO_04658* genes into pGEM-Teasy vector following PCR. The *detR* and *PXO_04658* fragments were then subcloned into the pUC18 vector to generate pUCdetR and pUC04658 plasmids using *Nde*I–*Bam*HI and *Eco*RI, respectively. To generate the knockout constructs pUCdetR$^-$ and pUC04685$^-$, the plasmids were restricted with *Hin*cII for pUCdetR and *Msc*I for pUC04658, and ligated with the kanamycin resistance cassette, which was isolated from pGEMKm following digestion with *Hin*cII. Knockout constructs were introduced into PXO99 competent cells by electroporation and knockout strains were selected as reported previously by Lee and Ronald (2007).

Generation of complementary strain, C*detR*$^-$

To verify possible polar effects of the *detR*$^-$ knockout, we produced the complementary strain C*detR*$^-$ constitutively expressing the DetR protein with a 6 × His-tag at its N-terminus under the control of the *lac* promoter on the pBBR1-MCS5 vector (Fig. S2). Full-length *detR* was amplified using the primer set CdetR_N_His, which contained a 6 × His-tag on the forward primer, and cloned into a pGEM-Teasy vector. The 6 × *His-detR* fragment was sequenced and subcloned into the broad-host-range vector pBBR1-MCS5 using *Eco*RI–*Bam*HI. The resulting construct was introduced into *detR*$^-$ competent cells by electroporation, and complementary strains were selected on PSA containing 10 μg/mL gentamycin.

Virulence assays

To determine the virulence of RR knockout strains, we infected TP309 leaves with bacteria by the scissor clipping method (Chelikani *et al*., 2004). Specifically, *Xoo* strains were cultured on PSA containing cephalexin (for PXO99), kanamycin (for *detR*$^-$ and *PXO_04658*$^-$) or gentamycin (for C*detR*$^-$) at 28 °C for 3 days. The bacteria were suspended in distilled water to achieve a population of 10^7 CFU/mL. Bacterial suspensions were used to infect rice leaves and lesion lengths were measured at 14 dpi. The average bacterial population per square centimetre of infected leaves was determined by the following procedure. At the zero time point (immediately after infection), 1-cm^2 samples from the infected site of three leaves were cut and placed into 1 mL of sterile distilled water containing cephalexin to measure the bacterial population bound to the leaves (Lee *et al*., 2008b). For other time points, inoculated leaves were sterilized in 0.5% sodium hypochlorite solution for 2 min (Das *et al*., 2009) and 4-cm^2 (for 0.5, 1, 2, 3 hpi) or 25-cm^2 (for 14 dpi) samples from the infected site of three leaves were sliced into small pieces, incubated in 1 or 10 mL sterile distilled water containing 15 μg/mL of cephalexin, respectively, and shaken for 1 h. The suspensions of extracted bacteria were diluted and plated onto PSA. The colonies on the plates were counted after 3 days of

incubation at 28 °C. These results were calculated to obtain the average bacterial population per square centimetre of infected leaves (CFU/cm^2), as shown in Figs 1B and S5.

Quantification of EPS by the sulfuric–phenol colorimetric method

Xoo strains [at an initial optical density at 600 nm (OD_{600}) of 0.1] were grown in 20 mL TGY containing 5 g/L tryptone, 5 g/L glucose, 3 g/L yeast extract, 700 mg/L K_2HPO_4 and 250 mg/L $MgSO_4.7H_2O$ (Haynes *et al*., 1955) for 5 days to achieve the maximum amount of EPS (Vojnov *et al*., 2001). EPS was extracted from the supernatant by ethanol precipitation and measured by the sulfuric–phenol colorimetric method at 490 nm, as described previously (Kumar and Sakthivel, 2001), using a spectrophotometer (UV Spectrophotometer UV1800 Shimadzu, Nakagyo-ku, Kyoto, Japan). A standard curve was created using a mixture of D-glucose, D-mannose and D-glucuronic acid (ratio 5 : 5 : 2) for quantification of *Xoo* EPS (Misaki *et al*., 1962).

Siderophore assay

To observe changes in iron homeostasis of *Xoo* strains, we performed siderophore assays (Schwyn and Neilands, 1987) as described previously, but using PSA instead of minimal medium (Chatterjee and Sonti, 2002). Specifically, bacteria grown on PSA plates were harvested, washed three times with sterile distilled water to remove EPS and suspended in water. Bacterial samples (10 μL, 10^8 CFU) were dropped onto PSA-CAS (iron-rich) and PSA-CAS-DP (iron-limited) media. The halo zone on the media was checked at 1 days after inoculation (dai) for PSA-CAS-DP and at 2 dai for PSA-CAS.

Growth curve of *Xoo* strains in iron-rich and iron-limited conditions

To examine the growth pattern of *Xoo* strains under iron-dependent conditions, approximately 10^3 CFU/mL of bacterial population were grown at 28 °C in 50 mL of fresh PSB containing 9 μM $FeCl_3$ for iron-rich conditions or 100 μM DP for iron-limited conditions (Pandey and Sonti, 2010), and shaken at 150 rpm for 4 days. One millilitre of the bacterial cultures was taken every 24 h and diluted to count the cell population.

Tolerance to H_2O_2

To examine the ability to detox ROS, we investigated the H_2O_2 tolerance of *Xoo* strains. After 2 days of growth, bacterial colonies grown on PSA plates were scraped into 1.5-mL tubes and washed three times with sterile distilled water. Cells were suspended in PSB containing different concentrations of H_2O_2 at a density of 10^8 CFU/mL and then shaken at 200 rpm and 28 °C for 1 h. The cells were pelleted, washed three times with sterile distilled water and aliquots were dropped onto PSA to count cell numbers.

Catalase activity assay

To determine the activity of detoxifying enzyme, we performed the catalase activity assay as reported previously (Subramoni and Sonti, 2005). *Xoo* strains were grown to late-logarithmic phase in PSB with suitable antibiotics, and then 15 mL of bacteria were added to 300 mL fresh PSB with or without 0.5 mM H_2O_2 and shaken at 150 rpm and 28 °C for 2 h. Bacterial cells were harvested by centrifugation (4,800×*g*, 10 min, 4 °C), washed three times with distilled water to remove EPS and resuspended in 50 mM potassium phosphate buffer containing 0.1 mM ethylenediaminetetraacetic acid (EDTA). The cell suspensions were sonicated for 2 min (30% amplitude, 5-s pulse on, 10-s pulse off) on ice, and cell debris was removed by centrifugation (14,000×*g*, 10 min, 4 °C). Total protein concentration was measured according to the Bradford method (Bradford, 1976) with bovine serum albumin as a standard. Catalase activity was assayed from the rate of H_2O_2 decomposition, as measured by decreased absorbance at 240 nm, following the procedure of Aebi (1974). The reaction mixture contained 50 mM potassium phosphate buffer (pH 7.0) and 100 μg of total protein extract. The reaction was initiated by the addition of 10 mM H_2O_2. The specific activity of catalase was calculated using the following equation:

$$\text{Specific activity} = \frac{V}{\varepsilon \times d \times v \times C} \times \frac{\Delta E}{\Delta t}$$

where V is the total reaction volume (mL), ε is the extinction coefficient (40 mmol/L/cm), d is the light path (1 cm), v is the volume of protein (mL), C is the concentration of protein (mg/mL) and $\Delta E/\Delta t$ is the change in A_{240} in 1 min.

RNA extraction

RNA was extracted using RNAiso (Takara, Kusatsu, Shiga, Japan). The cell pellet was suspended in 300 μL of diethylpyrocarbonate (DEPC)-treated distilled water and sonicated for 3 min (20% AMP, 5-s pulse on, 10-s pulse off) on ice. According to the Takara manual, 100 μL of cell lysate was mixed with 1 mL of RNAiso and RNA was extracted. The RNA pellet was suspended in 50 μL of DEPC-treated distilled water and its concentration was measured.

RT-PCR and real-time qRT-PCR

RT-PCR and real-time qRT-PCR were applied to compare the expression levels of various genes between PXO99 and *detR*$^-$. For genes associated with EPS, bacteria were harvested at the stationary phase in TGY. For genes related to iron homeostasis, bacteria were harvested at 2 dai on PSA-CAS and PSA-CAS-DP. For *in planta* experiments, bacteria were harvested from infected leaves at 6 days after infection using the method described by Soto-Suarez *et al*. (2010). RNA was extracted using RNAiso and 50 μg of RNA were treated with DNaseI (Takara) to eliminate genomic DNA. cDNA was synthesized from 4 μg of RNA using a Takara cDNA synthesis kit and random hexamer primers. Synthesized cDNA was diluted 10-fold and then used for RT-PCR or real-time qRT-PCR. *16S rRNA* was used as an internal control for RT-PCR and a reference gene for real-time qRT-PCR.

Real-time qRT-PCR was performed on a Rotor-Gene Q (Qiagen, Venlo, Netherlands). The reaction mixture (10 μL) contained 5 μL of SYBR Premix Ex Taq 2× (Takara), 1 μL of cDNA product (40 ng) and 2 μL of 10 pM specific primers (Table S5, see Supporting Information). PCR conditions

were 95 °C for 15 min, followed by 45 cycles of 95 °C for 15 s, 60 °C for 15 s and 72 °C for 15 s, with subsequent melting curve analysis. *16S rRNA* was used as an internal control for normalization and there were three replicates for each sample. The experiment was repeated three times independently. Gene expression levels were calculated using the $2^{-\Delta\Delta Ct}$ method (Livak and Schmittgen, 2001).

Domain analysis and promoter prediction

To predict the functional domains of DetR and PXO_04658 proteins, we used the web-based tool SMART (simple modular architecture research tool; http://smart.embl-heidelberg.de) (Schultz *et al*., 1998).

To predict the promoter region in the 196-nucleotide region between *detR* and *PXO_04658*, we applied BPROM, a bacterial sigma 70 promoter recognitions program (Solovyev and Salamov, 2011).

Statistical analysis

Statistically significant differences were analysed by Student's *t*-test or analysis of variance (ANOVA) followed by Duncan's test (Duncan, 1955). Significance was set at $P < 0.001$, $P < 0.01$ and $P < 0.05$ and was determined using SPSS Software.

ACKNOWLEDGEMENTS

The authors declare that they have no competing interests.

This research was supported by the Basic Science Research Program through the National Research Foundation of Korea (NRF) funded by the Ministry of Education (NRF-2013R1A1A2009726).

REFERENCES

Abdul-Tehrani, H., Hudson, A.J., Chang, Y.-S., Timms, A.R., Hawkins, C., Williams, J.M., Harrison, P.M., Guest, J.R. and Andrews, S.C. (1999) Ferritin mutants of *Escherichia coli* are iron deficient and growth impaired, and *fur* mutants are iron deficient. *J. Bacteriol*. **181**, 1415–1428.

Aebi, H. (1974) Catalases. *Methods Enzym. Anal*. **2**, 673–684.

Andrews, S.C., Robinson, A.K. and Rodríguez-Quiñones, F. (2003) Bacterial iron homeostasis. *FEMS Microbiol. Rev*. **27**, 215–237.

Aslam, S.N., Newman, M.-A., Erbs, G., Morrissey, K.L., Chinchilla, D., Boller, T., Jensen, T.T., De Castro, C., Ierano, T., Molinaro, A., Jackson, R.W., Knight, M.R. and Cooper, R.M. (2008) Bacterial polysaccharides suppress induced innate immunity by calcium chelation. *Curr. Biol*. **18**, 1078–1083.

Auh, C.-K. and Murphy, T.M. (1995) Plasma membrane redox enzyme is involved in the synthesis of O_2^- and H_2O_2 by *Phytophthora* elicitor-stimulated rose cells. *Plant Physiol*. **107**, 1241–1247.

Ausubel, F., Brent, R., Kingston, R., Moore, D., Seidman, J., Smith, J. and Struhl, K. (1994) *Current Protocols in Molecular Biology*. New York, NY: John Wiley & Sons.

Barakat, M., Ortet, P. and Whitworth, D.E. (2011) P2CS: a database of prokaryotic two-component systems. *Nucleic Acids Res.* **39**, D771–D776.

Barber, C., Tang, J., Feng, J., Pan, M., Wilson, T., Slater, H., Dow, J.M., Williams, P., and Daniels, M.J. (1997) A novel regulatory system required for pathogenicity of *Xanthomonas campestris* is mediated by a small diffusible signal molecule. *Mol. Microbiol*. **24**, 555–566.

Becker, A., Katzen, F., Puhler, A. and Ielpi, L. (1998) Xanthan gum biosynthesis and application: a biochemical/genetic perspective. *Appl. Microbiol. Biotechnol*. **50**, 145–152.

Bradford, M.M. (1976) A rapid and sensitive method for the quantitation of microgram quantities of protein utilizing the principle of protein–dye binding. *Anal. Biochem.* **72**, 248–254.

Branda, S.S., Vik, Å., Friedman, L. and Kolter, R. (2005) Biofilms: the matrix revisited. *Trends Microbiol*. **13**, 20–26.

Burdman, S., Shen, Y., Lee, S.W., Xue, Q. and Ronald, P. (2004) RaxH/RaxR: a two-component regulatory system in *Xanthomonas oryzae* pv. *oryzae* required for AvrXa21 activity. *Mol. Plant–Microbe Interact*. **17**, 602–612.

Büttner, D. and Bonas, U. (2010) Regulation and secretion of *Xanthomonas* virulence factors. *FEMS Microbiol. Rev*. **34**, 107–133.

Chamnongpol, S., Mongkolsuk, S., Vattanaviboon, P. and Fuangthong, M. (1995) Unusual growth phase and oxygen tension regulation of oxidative stress protection enzymes, catalase and superoxide dismutase, in the phytopathogen *Xanthomonas oryzae* pv. *oryzae*. *Appl. Environ. Microbiol*. **61**, 393–396.

Chatterjee, S. and Sonti, R.V. (2002) *rpfF* mutants of *Xanthomonas oryzae* pv. *oryzae* are deficient for virulence and growth under low iron conditions. *Mol. Plant–Microbe Interact*. **15**, 463–471.

Chelikani, P., Fita, I. and Loewen, P. (2004) Diversity of structures and properties among catalases. *Cell. Mol. Life Sci*. **61**, 192–208.

Cho, H.-J., Park, Y.-J., Noh, T.-H., Kim, Y.-T., Kim, J.-G., Song, E.-S., Lee, D.H. and Lee, B.M. (2008) Molecular analysis of the *hrp* gene cluster in *Xanthomonas oryzae* pathovar *oryzae* KACC10859. *Microb. Pathog.* **44**, 473–483.

Das, A., Rangaraj, N. and Sonti, R.V. (2009) Multiple adhesin-like functions of *Xanthomonas oryzae* pv. *oryzae* are involved in promoting leaf attachment, entry, and virulence on rice. *Mol. Plant–Microbe Interact*. **22**, 73–85.

Dat, J., Vandenabeele, S., Vranová, E., Van Montagu, M., Inzé, D. and Van Breusegem, F. (2000) Dual action of the active oxygen species during plant stress responses. *Cell. Mol. Life Sci*. **57**, 779–795.

Denny, T. (1995) Involvement of bacterial polysaccharides in plant pathogenesis. *Annu. Rev. Phytopathol*. **33**, 173–197.

Doke, N. (1983) Involvement of superoxide anion generation in the hypersensitive response of potato tuber tissues to infection with an incompatible race of *Phytophthora infestans* and to the hyphal wall components. *Physiol. Plant Pathol*. **23**, 345–357.

Duncan, D.B. (1955) Multiple range and multiple F tests. *Biometrics*, **11**, 1–42.

Froger, A. and Hall, J.E. (2007) Transformation of plasmid DNA into *E. coli* using the heat shock method. *J. Vis. Exp.* **253**.

Grant, M., Brown, I., Adams, S., Knight, M., Ainslie, A. and Mansfield, J. (2000) The RPM1 plant disease resistance gene facilitates a rapid and sustained increase in cytosolic calcium that is necessary for the oxidative burst and hypersensitive cell death. *Plant J*. **23**, 441–450.

Haynes, W., Wickerham, L. and Hesseltine, C. (1955) Maintenance of cultures of industrially important microorganisms. *Appl. Microbiol*. **3**, 361–368.

He, Y.-W., Wu, J.E., Cha, J.-S. and Zhang, L.-H. (2010) Rice bacterial blight pathogen *Xanthomonas oryzae* pv. *oryzae* produces multiple DSF-family signals in regulation of virulence factor production. *BMC Microbiol*. **10**, 187.

Jansson, P.-E., Kenne, L. and Lindberg, B. (1975) Structure of the extracellular polysaccharide from *Xanthomonas campestris*. *Carbohydr. Res.* **45**, 275–282.

Jeong, K.S., Lee, S.E., Han, J.W., Yang, S.U., Lee, B.M., Noh, T.H. and Cha, J.S. (2008) Virulence reduction and differing regulation of virulence genes in *rpf* mutants of *Xanthomonas oryzae* pv. *oryzae*. *Plant Pathol. J*. **24**, 143–151.

Jha, G., Rajeshwari, R. and Sonti, R.V. (2007) Functional interplay between two *Xanthomonas oryzae* pv. *oryzae* secretion systems in modulating virulence on rice. *Mol. Plant–Microbe Interact*. **20**, 31–40.

Katzen, F., Becker, A., Zorreguieta, A., Pühler, A. and Ielpi, L. (1996) Promoter analysis of the *Xanthomonas campestris* pv. *campestris gum* operon directing biosynthesis of the xanthan polysaccharide. *J. Bacteriol*. **178**, 4313–4318.

Katzen, F., Ferreiro, D.U., Oddo, C.G., Ielmini, M.V., Becker, A., Pühler, A. and Ielpi, L. (1998) *Xanthomonas campestris* pv. *campestris gum* mutants: effects on xanthan biosynthesis and plant virulence. *J. Bacteriol*. **180**, 1607–1617.

Kim, S.Y., Kim, J.G., Lee, B.M. and Cho, J.Y. (2009) Mutational analysis of the *gum* gene cluster required for xanthan biosynthesis in *Xanthomonas oryzae* pv *oryzae*. *Biotechnol. Lett*. **31**, 265–270.

Kovach, M.E., Elzer, P.H., Steven Hill, D., Robertson, G.T., Farris, M.A., Roop Ii, R.M. and Peterson, K.M. (1995) Four new derivatives of the broad-host-range cloning vector pBBR1MCS, carrying different antibiotic-resistance cassettes. *Gene*, **166**, 175–176.

Kumar, R.S. and Sakthivel, N. (2001) Exopolysaccharides of *Xanthomonas* pathovar strains that infect rice and wheat crops. *Appl. Microbiol. Biotechnol*. **55**, 782–786.

Lamb, C. and Dixon, R.A. (1997) The oxidative burst in plant disease resistance. *Annu. Rev. Plant Physiol. Plant Mol. Biol*. **48**, 251–275.

Laub, M.T. and Goulian, M. (2007) Specificity in two-component signal transduction pathways. *Annu. Rev. Genet*. **41**, 121–145.

Lee, B.-M., Park, Y.-J., Park, D.-S., Kang, H.-W., Kim, J.-G., Song, E.-S., Park, I.C., Yoon, U.H., Hahn, J.H., Koo, B.S., Lee, G.B., Kim, H., Park, H.S., Yoon, K.O., Kim, J.H., Jung, C.H., Koh, N.H., Seo, J.S. and Go, S.J. (2005) The genome sequence of *Xanthomonas oryzae* pathovar *oryzae* KACC10331, the bacterial blight pathogen of rice. *Nucleic Acids Res*. **33**, 577–586.

Lee, C.-K., Lee, B.-M. and Cho, J.-Y. (2008a) Identification of new internal promoters of the *Xanthomonas oryzae* pathovar *oryzae gum* gene cluster. *Biotechnol. Lett*. **30**, 521–527.

Lee, S.-W. and Ronald, P.C. (2007) Marker-exchange mutagenesis and complementation strategies for the gram-negative bacteria *Xanthomonas oryzae* pv. *oryzae*. In: *Plant–Pathogen Interactions* (Ronald, P.C., ed.), pp. 11–18, New York: Humana press.

Lee, S.W., Jeong, K.S., Han, S.W., Lee, S.E., Phee, B.K., Hahn, T.R. and Ronald, P. (2008b) The *Xanthomonas oryzae* pv. *oryzae* PhoPQ two-component system is required for AvrXA21 activity, *hrpG* expression, and virulence. *J. Bacteriol*. **190**, 2183–2197.

Li, J. and Wang, N. (2011) The *wxacO* gene of *Xanthomonas citri* ssp. *citri* encodes a protein with a role in lipopolysaccharide biosynthesis, biofilm formation, stress tolerance and virulence. *Mol. Plant Pathol*. **12**, 381–396.

Liang, S., Yang, F., Guan, W., Wu, M., Chen, H., Tian, F., Xu, Y. and He, C. (2011) Gene deletion and functional analysis of the EAL domain protein *vieAxoo* in *Xanthomonas oryzae* pv. *oryzae*. *Wei Sheng Wu Xue Bao* **51**, 29–34.

Livak, K.J. and Schmittgen, T.D. (2001) Analysis of relative gene expression data using real-time quantitative PCR and the $2^{-\Delta\Delta CT}$ method. *Methods*, **25**, 402–408.

Misaki, A., Kirkwood, S., Scaletti, J. and Smith, F. (1962) Structure of the extracellular polysaccharide produced by *Xanthomonas oryzae*. *Can. J. Chem*. **40**, 2204–2213.

Ochiai, H., Inoue, Y., Takeya, M., Sasaki, A. and Kaku, H. (2005) Genome sequence of *Xanthomonas oryzae* pv. *oryzae* suggests contribution of large numbers of effector genes and insertion sequences to its race diversity. *Jpn. Agric. Res. Q*. **39**, 275–287.

Pandey, A. and Sonti, R.V. (2010) Role of the FeoB protein and siderophore in promoting virulence of *Xanthomonas oryzae* pv. *oryzae* on rice. *J. Bacteriol*. **192**, 3187–3203.

Pollock, T.J., Thorne, L., Yamazaki, M., Mikolajczak, M.J. and Armentrout, R.W. (1994) Mechanism of bacitracin resistance in gram-negative bacteria that synthesize exopolysaccharides. *J. Bacteriol*. **176**, 6229–6237.

Ray, S.K., Rajeshwari, R. and Sonti, R.V. (2000) Mutants of *Xanthomonas oryzae* pv. *oryzae* deficient in general secretory pathway are virulence deficient and unable to secrete xylanase. *Mol. Plant–Microbe Interact*. **13**, 394–401.

Repine, J., Fox, R.B. and Berger, E. (1981) Hydrogen peroxide kills *Staphylococcus aureus* by reacting with staphylococcal iron to form hydroxyl radical. *J. Biol. Chem*. **256**, 7094–7096.

Salzberg, S.L., Sommer, D.D., Schatz, M.C., Phillippy, A.M., Rabinowicz, P.D., Tsuge, S., Furutani, A., Ochiai, H., Delcher, A.L., Kelley, D., Madupu, R., Puiu, D., Radune, D., Shumway, M., Trapnell, C., Aparna, G., Jha, G., Pandey, A., Patil, P.B., Ishihara, H., Meyer, D.F., Szurek, B., Verdier, V., Koebnik, R., Dow, J.M., Ryan, R.P., Hirata, H., Tsuyumu, S., Sang Won, L., Ronald, P.C., Sonti, R.V., Van Sluys, M.A., Leach, J.E., White, F.F., and Bogdanove, A.J. (2008) Genome sequence and rapid evolution of the rice pathogen *Xanthomonas oryzae* pv. *oryzae* PXO99A. *BMC Genomics*, **9**, 204.

Sambrook, J. and Russell, D. (2001) Molecular Cloning: A Laboratory Manual. Cold Spring Harbor, New York: Cold Spring Harbor Laboratory Press.

Schultz, J., Milpetz, F., Bork, P. and Ponting, C.P. (1998) SMART, a simple modular architecture research tool: identification of signaling domains. *Proc. Natl. Acad. Sci. USA*, **95**, 5857–5864.

Schwyn, B. and Neilands, J.B. (1987) Universal chemical assay for the detection and determination of siderophores. *Anal. Biochem*. **160**, 47–56.

Shen, Y. and Ronald, P. (2002) Molecular determinants of disease and resistance in interactions of *Xanthomonas oryzae* pv. *oryzae* and rice. *Microbes Infect*. **4**, 1361–1367.

Solovyev, V. and Salamov, A. (2011) Automatic annotation of microbial genomes and metagenomic sequences. Metagenomics and its applications. In: *Agriculture, Biomedicine and Environmental Studies* (Li, R.W., ed.), pp. 61–78, New York: Nova Science Publishers.

Soto-Suarez, M., Bernal, D., Gonzalez, C., Szurek, B., Guyot, R., Tohme, J. and Verdier, V. (2010) *In planta* gene expression analysis of *Xanthomonas oryzae* pathovar *oryzae*, African strain MAI1. *BMC Microbiol*. **10**, 170.

Subramoni, S. and Sonti, R.V. (2005) Growth deficiency of a *Xanthomonas oryzae* pv. *oryzae fur* mutant in rice leaves is rescued by ascorbic acid supplementation. *Mol. Plant–Microbe Interact*. **18**, 644–651.

Subramoni, S., Pandey, A., Vishnu Priya, M.R., Patel, H.K. and Sonti, R.V. (2012) The ColRS system of *Xanthomonas oryzae* pv. *oryzae* is required for virulence and growth in iron-limiting conditions. *Mol. Plant Pathol*. **13**, 690–703.

Sutherland, I.W. (2001) The biofilm matrix–an immobilized but dynamic microbial environment. *Trends Microbiol*. **9**, 222–227.

Touati, D., Jacques, M., Tardat, B., Bouchard, L. and Despied, S. (1995) Lethal oxidative damage and mutagenesis are generated by iron in Δ*fur* mutants of *Escherichia coli*: protective role of superoxide dismutase. *J. Bacteriol*. **177**, 2305–2314.

Vanderslice, R., Doherty, D., Capage, M., Betlach, M., Hassler, R., Henderson, N., Ryan-Graniero, J. and Tecklenburg, M. (1989) Genetic engineering of polysaccharide structure in *Xanthomonas campestris*. In: *Biomedical and Biotechnological Advances in Industrial Polysaccharides* (Crescenzi, V., Dea, I.C.M., Paoletti, S., Stivala, S.S., Sutherland, I.W., ed.), pp. 145–156, New York: Gordon and Breach Science Publishers.

Vojnov, A.A., Slater, H., Daniels, M.J. and Dow, J.M. (2001) Expression of the *gum* operon directing xanthan biosynthesis in *Xanthomonas campestris* and its regulation in planta. *Mol. Plant–Microbe Interact*. **14**, 768–774.

Wang, F.-F., Wang, L. and Qian, W. (2010) Two-component signal transduction systems and regulation of virulence factors in *Xanthomonas*: a perspective. *Front. Biol*. **5**, 495–506.

West, A.H. and Stock, A.M. (2001) Histidine kinases and response regulator proteins in two-component signaling systems. *Trends Biochem. Sci*. **26**, 369–376.

White, F.F., Potnis, N., Jones, J.B. and Koebnik, R. (2009) The type III effectors of *Xanthomonas*. *Mol. Plant Pathol*. **10**, 749–766.

Williams, R.H. and Whitworth, D.E. (2010) The genetic organisation of prokaryotic two-component system signalling pathways. *BMC Genomics*, **11**, 720.

Winterbourn, C.C. (1995) Toxicity of iron and hydrogen peroxide: the Fenton reaction. *Toxicol. Lett*. **82**, 969–974.

Yun, M.H., Torres, P.S., El Oirdi, M., Rigano, L.A., Gonzalez-Lamothe, R., Marano, M.R., Castagnaro, A.P., Dankert, M.A., Bouarab, K. and Vojnov, A.A. (2006) Xanthan induces plant susceptibility by suppressing callose deposition. *Plant Physiol*. **141**, 178–187.

SUPPORTING INFORMATION

Additional Supporting Information may be found in the online version of this article at the publisher's website:

Methods S1 Purification of His-DetR recombinant protein. *Xanthomonas oryzae* pv. *oryzae* (*Xoo*) strains were cultured in 100 mL peptone sucrose broth (PSB) containing suitable antibiotics until the stationary phase. Cells were harvested by centrifugation (9,700×*g*, 30 min, 4 °C), washed with 100 mL distilled water and harvested again with the same centrifugation conditions. Cell pellets were suspended in 25 mL of lysis buffer (50 mM NaH_2PO_4, 300 mM NaCl, 10 mM imidazole, pH 8.0) containing 20 μL of lysozyme (400 000 U/mL). After incubation overnight at 4 °C, cells were sonicated for 5 min (40% amplitude, 5-s pulse on, 10-s pulse off) on ice and then centrifuged (14,000×*g*, 30 min, 4 °C). The supernatant was filtered through a 0.2-μm filter to remove all cell debris. The purification column was packed with 100 μL of Ni-NTA agarose (Qiagen, Venlo, Netherlands) and the lysate was purified according to the manufacturer's instructions. The column was washed with washing buffer (50 mM NaH_2PO_4, 300 mM NaCl, 20 mM imidazole, pH 8.0). In the last step, binding proteins were eluted by 500 μL of elution buffer (50 mM NaH_2PO_4, 300 mM NaCl, 500 mM imidazole, pH 8.0). The target protein was verified by sodium dodecylsulfate-polyacrylamide gel electropho-

resis (SDS-PAGE) and Western blotting with histidine (His) probe (Novagen, Darmstadt, Germany) as the primary antibody and horseradish peroxidase (HRP) probe (Santa cruz biotechnology, Dallas, Texas, USA) as the secondary antibody. PXO99 and *detR*$^-$ were used as negative controls to confirm the expression of 6 × His-DetR in C*detR*$^-$.

Methods S2 Growth curves of *Xanthomonas oryzae* pv. *oryzae* (*Xoo*) strains in peptone sucrose broth (PSB). A single colony of each *Xoo* strain was grown in 5 mL of PSB containing suitable antibiotics. When the cultures reached the stationary phase, bacteria were added to 50 mL of PSB with 15 μg/mL cephalexin to give a starting population of 10^4 colony-forming units (CFU)/mL, and shaken at 150 rpm and 28 °C. Growth of the bacterial population was measured by colony counting every 12 h for 4 days.

Methods S3 Quantification of colony-forming units (CFU) per colony of PXO99 and *detR*$^-$. A single colony of each *Xoo* strain grown on peptone sucrose agar (PSA) containing suitable antibiotics was taken and suspended with 200 μL of distilled water. The colony suspension was re-inoculated with dilution on PSA containing suitable antibiotics, incubated at 28 °C for 3 days and the colonies were counted. This experiment was carried out with three colonies for each strain and was performed twice with similar results.

Fig. S1 Overview of DetR and PXO_04658 including the genetic map and the functional domains, and their position on the amino acid sequence.

Fig. S2 The complementary strain C*detR*$^-$ constitutively expresses 6 × His-DetR recombinant protein.

Fig. S3 Growth curves of PXO99 and *detR*$^-$ in peptone sucrose broth (PSB).

Fig. S4 Comparison of gene expression between PXO99 and *detR*$^-$ by reverse transcription-polymerase chain reaction (RT-PCR).

Fig. S5 Bacterial population during the initial hours after infection.

Fig. S6 H_2O_2 threshold of PXO99 and *detR*$^-$.

Fig. S7 Reverse transcription-polymerase chain reaction (RT-PCR) of 49 response regulators (RRs) and hybrid histidine kinase-response regulators (HyHKs) showed insignificant differences between PXO99 and *detR*$^-$ *in planta*.

Fig. S8 Reverse transcription-polymerase chain reaction (RT-PCR) of 64 transcription factors (TFs) showed insignificant differences between PXO99 and *detR*$^-$ *in planta*.

Fig. S9 Comparison of phenotypes between PXO99, *detR*$^-$ and *PXO_04658*$^-$.

Table S1 Primers for the generation of knockout mutant and complementary strains.

Table S2 Primers for reverse transcription-polymerase chain reaction (RT-PCR) of virulence factor genes.

Table S3 Primers for reverse transcription-polymerase chain reaction (RT-PCR) of PXO99 response regulator (RR) and hybrid histidine kinase-response regulator (HyHK) genes.

Table S4 Primers for reverse transcription-polymerase chain reaction (RT-PCR) of PXO99 transcription factor (TF) genes.

Table S5 Primers for real-time quantitative reverse transcription-polymerase chain reaction (RT-PCR) of virulence factor (VF) genes.